



Design and synthesis of novel phe-phe hydroxyethylene derivatives as potential coronavirus main protease inhibitors

Zahra Khorsandi^a, Maral Afshinpour^b, Fatemeh Molaei^c, Rafee Habib Askandar^d, Fariba Keshavarzipour^e, Maryam Abbasi^f  and Hojjat Sadeghi-Aliabadi^g

^aDepartment of Chemistry, Isfahan University of Technology, Isfahan, Iran; ^bBioinformatics Lab., Department of Biology, School of Sciences, Razi University, Kermanshah, Iran; ^cDepartment of Anaesthesiology, Faculty of Paramedical, Jahrom University of medical science, Jahrom, Iran; ^dResearch Center, Sulaimani Polytechnic University, Sulaimani, Iraq; ^eIsfahan Pharmaceutical Sciences Research Center, School of Pharmacy, Isfahan University of Medical Sciences, Isfahan, Iran; ^fDepartment of Medicinal Chemistry, Faculty of Pharmacy, Hormozgan University of Medical Sciences, Bandar Abbas, Iran; ^gDepartment of Medicinal Chemistry, Faculty of Pharmacy, Isfahan University of Medical Sciences, Isfahan, Iran

Communicated by Ramaswamy H. Sarma

ABSTRACT

In response to the current pandemic caused by the novel SARS-CoV-2, we design new compounds based on Lopinavir structure as an FDA-approved antiviral agent which is currently under more evaluation in clinical trials for COVID-19 patients. This is the first example of the preparation of Lopinavir isosteres from the main core of Lopinavir conducted to various heterocyclic fragments. It is proposed that main protease inhibitors play an important role in the cycle life of coronavirus. Thus, the protease inhibition effect of synthesized compounds was studied by molecular docking method. All of these 10 molecules, showing a good docking score compared. Molecular dynamics (MD) simulations also confirmed the stability of the best-designed compound in Mpro active site.

ARTICLE HISTORY

Received 18 October 2020
Accepted 15 March 2021

KEYWORDS

Covid-19; lopinavir; molecular docking; molecular dynamic simulation; synthesis

Introduction

In recent months, the pandemic of novel Coronavirus (COVID-19) is spreading around the world. The number of confirmed cases at the time of writing this manuscript (4 January 2021) exceeded 83,910,386 and there were confirmed more than 1,839,660 deaths (WHO, 2020).

COVID-19 is a member of human beta coronaviruses which also include SARS and MERS (Elfiky et al., 2017). The mortality rates for SARS and MERS HCoV are more than COVID-19 (10% and 36%, respectively in comparison with 2–3%) but the spreading rate of the new virus is amazing in a few months (Hemida & Alnaeem, 2019; WHO, 2016)


Screening of existing antiviral drugs was known as a fast and useful strategy against SARS-CoV-2; thus, considering to pandemic of COVID-19 and time-consuming of the drug discovery process, finding a new compound against the virus drug via repurposing seems like a logical and essential strategy; however, drug discovery progression has to start somewhere. For further evaluations and founding new drugs for the treatments of COVID-19, focusing on the chemical structure of available drugs against other viruses including the similar SARS-CoV, middle east respiratory syndrome coronavirus (MERS-CoV), human immunodeficiency virus (HIV), and hepatitis C virus (HCV) have been suggested (Cunningham et al., 2020; Ko et al., 2020; Zhou et al., 2020).

For instance, the commonly used HIV treatment is based on main protease (Mpro/chymotrypsin-like protease (3CLpro)) inhibitors such as Lopinavir/Ritonavir which was applied as a preliminary candidate for the treatment of COVID-19 infected patients (Morales et al., 2020). This protease displays a potential target for the inhibition of CoV replication.

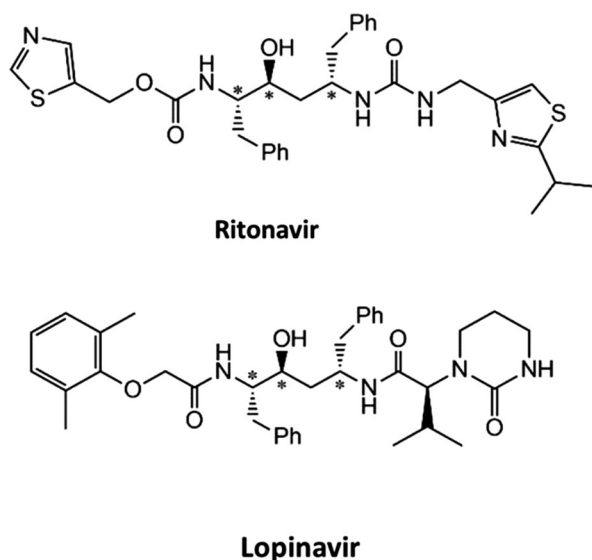
In recent months, numerous researches have been reported to determine the effective inhibitors for SARS-CoV-2 through in-silico docking models (Ghosh et al., 2020; Kadil et al., 2020). Also, several antiviral medications such as Lopinavir, Zanamivir, Indinavir, Saquinavir, and Remdesivir display potential as main proteases and as a treatment for COVID-19 (Hall & Ji, 2020). More importantly, the beneficial of some compounds such as Lopinavir was proven for the treatment of SARS-CoV-2 infections on clinical trials. Most of known main proteases have a similar shape which matches the capacity of the receptor active site. For example, the core unit of Lopinavir and Ritonavir is L-phenylalanine (phe-phe hydroxyethylene isostere) which in this study, their amino group is functionalized with the different organic unit (Scheme 1).

Considering to progressively application of these chemical compounds as protease inhibitors, we design novel protease inhibitors based on Lopinavir structure and introduce a short and efficient synthesis method for their preparation. Although several methods have been developed for the synthesis of these dipeptide derivatives, herein, we have afforded to

CONTACT Maryam Abbasi  mabbasi@hums.ac.ir  Department of Medicinal Chemistry, Faculty of Pharmacy, Hormozgan University of Medical Sciences, Bandar Abbas, Iran; Hojjat Sadeghi-Aliabadi  sadeghi@pharm.mui.ac.ir  Department of Medicinal Chemistry, Faculty of Pharmacy, Isfahan University of Medical Sciences, Isfahan, Iran

 Supplemental data for this article can be accessed online at <https://doi.org/10.1080/07391102.2021.1905549>.

© 2021 Informa UK Limited, trading as Taylor & Francis Group



Scheme 1. Chemical structures of Lopinavir and Ritonavir

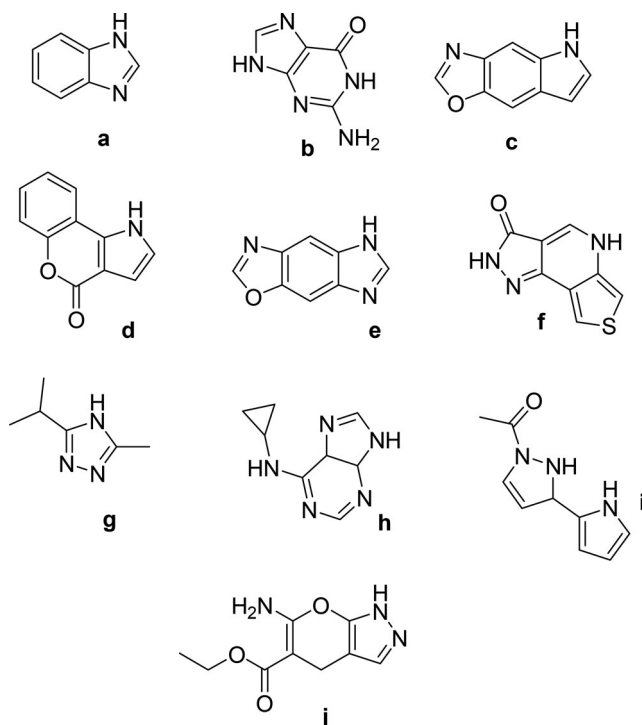
the presented practical strategy which behind disadvantages of commonly available approaches such as multi-complex steps, harsh reaction condition and low yields of products (Bhaskar et al., 2008; Damo et al., 2006). In continuous, the main proteases-inhibiting potential of synthesized compounds was investigated using computational studies including molecular docking and molecular dynamics simulation.

Fragment-based drug design is a general method to design new compounds which have introduced as an impressive substitute to high throughput screening of compounds in drug discovery (Kumar et al., 2012; Murray & Blundell, 2010). In this approach, fragments as small organic moieties such as active heterocyclic rings are fused to the main pharmacophore. Some new anticancer, anti-alzheimer, and anti-malarial agents have been developed via such process (Tănase et al., 2014).

Herein, to design new structures, some heterocyclic fragments were connected to the amino group of phe-phe hydroxyethylene core. Through our basic knowledge of protease inhibitors, the hydrogen bond potential and a high degree of hydrophobicity make more efficient in the blocking process (Sgrignani & Magistrat, 2012; Speck-Planche et al., 2012; Suvannang et al., 2011). Therefore, we applied non-toxic heterocyclic fragments which are known as the most important fragments in medical chemistry; their structure was given in Scheme 2.

The reported fragments are seen in different compounds, for example, guanine is one of the four main nucleobases found in the nucleic acids, DNA and RNA and characterized as potent immunosuppressive and chemotherapeutic agents (Scheme 2b) (Chern et al., 1993).

8H-oxazolo[4,5-g]indole has been reported as potent cytotoxic activities towards cancerous cell lines in diffuse malignant peritoneal mesothelioma (Scheme 2c,e). The chromeno[3,4-b]pyrrol-4(3H)-one framework is often existing in marine alkaloids such as ningalins and lamellarins (Scheme 2d). They also exhibit potent biological activities as immunomodulatory, anti-HIV-1, multidrug-resistant (MDR) reversal, phosphodiesterase-5 inhibitory (PDE-5) activities, and anti-analgesic behavior (Fan et al., 2008; Imbri et al., 2014). The



Scheme 2. Some heterocyclic fragments used in different pharmaceutical products

fused heterocyclic systems contain pyrazole (Scheme 2f) are among pharmacological importance compounds as inhibitors of HIV-1, pesticides, fungicides, antihypertensive and anti-cancer agents (Hassan et al., 1997; Min et al., 2006).

The 1,2,4-triazoles (Scheme 2g) has also attracted widespread attention due to their diverse applications as antibacterial, antidepressant, antiviral, antitumor, anti-inflammatory, pesticides, herbicides, dyes, lubricant, and analytical reagents (Dumas, 1999; Weng et al., 2012).

Also, purine derivatives (Scheme 2h) were introduced as antiviral agents and affect neuronal and muscle nicotinic acetylcholine receptors (Hřebabecký et al., 2012).

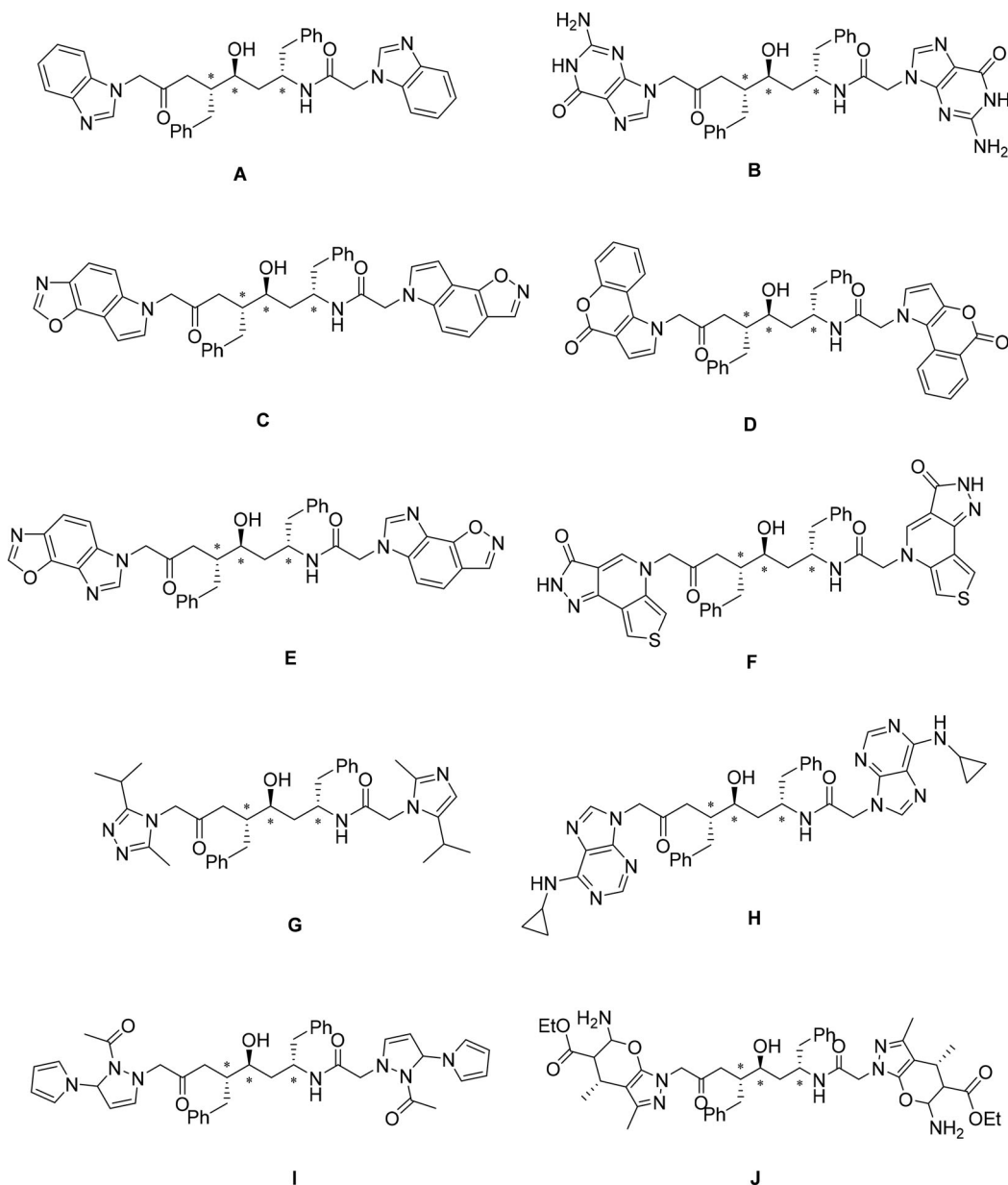
Pyranopyrazoles are other important class of heterocyclic compounds which have used as pharmaceutical constituents. Pyrano[2,3c]pyrazoles (Scheme 2i,j) have shown analgesic, anticancer, antitumor, and antiinflammatory activities (Khoobi et al., 2015).

In conclusion, these new designed structures as a potential of the COVID-19 main protease inhibition could be logical because they consist of a combination of known bioactive molecules and phe-phe hydroxyethylene scaffold which is the core of Lopinavir and Ritonavir as recommended drugs for the treatment of COVID-19 infected patients (Scheme 3). To confirm this opinion, the main interactions and binding energies of designed compounds were studied by molecular docking and molecular dynamics (MD) simulation.

Results and discussion

Synthesis

Herein, we would like to report a new green and economical synthesis of new proposed compounds. The synthesis



Scheme 3. Chemical structure of the new designed and synthesized compounds as COVID-19 main protease inhibitors.

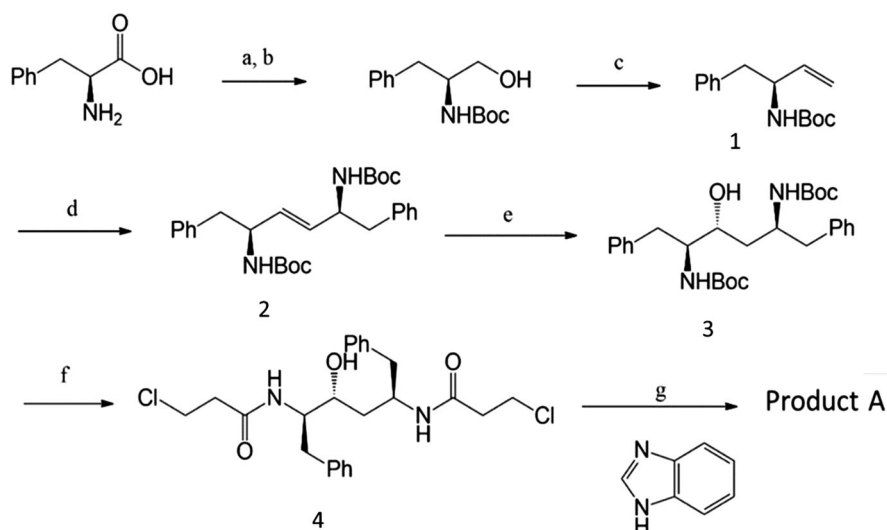
process was shown in [Scheme 4](#). Our general synthetic strategy is similar to that employed for Ritonavir according to the literature (Stoner et al., 2000).

This six-step procedure was applied to synthesized products in acceptable yields. Utilizing commonly available reagents and good reaction conditions, this process is sufficient for large-scale production and has been used to prepare these types of compounds in high yields (more than 85%).

As illustrated in [Scheme 4](#), the synthesis was started from commercially available L-phenyl alanine. L-phenyl alanine was protected with Boc and converted to its corresponding Boc-amino alcohol. The alcohol was oxidized to corresponding aldehyde and one carbon extension to olefin compound was occurred using standard Wittig reaction. These reactions were taken continuously without purification. The cross-metathesis reaction of olefin was done using Hoveyda-

Grubbs' second-generation olefin metathesis catalyst. Although, some reports for the synthesis of this olefin are available; they suffer from serious limitations such as more steps, using toxic and expensive reagents, and low yields of products. Therefore, to large scale synthesis, presentation more useful approach is valuable. The next step is hydroboration-oxidation reaction in presented Zn which gave final alcohol in excellent selectivity; it can be explained by a chelation control model. The synthesis of this pharmacy important core from phenylalanine has been reported previously which proceeds through a seven-step sequence using a large amount of metal catalyst.

After de-protection from amines, they were reacted with methyl 2-chloroacetate and various introduced amino heterocycles. The isolated yields of final products (which are shown in [Scheme 4](#)) were given in [Table 1](#). Details experimental were given in [supplemental data](#). Herein, we report a short



Scheme 4. Reaction of each step: (a) (i) AcCl , MeOH , reflux, 3 h; (ii) $(\text{Boc})_2\text{O}$, TEA , THF , r.t., 7 h; (b) LiCl , NaBH_4 , EtOH , THF , r.t., 16 h; (c) (i) PCC/charcoal , CH_2Cl_2 , r.t., 2 h; (ii) $\text{CH}_3\text{P}(\text{C}_6\text{H}_5)_3\text{Br}$, NaHMDS , -20°C , 40 min and at 20°C , 12 h (d) 10 mol % Hoveyda-Grubbs' second-generation catalyst, CH_2Cl_2 , 40°C 14 h; (e) $\text{Zn}(\text{BH}_4)_2$, H_2O_2 , NaOH , THF , 0 to r.t., 5 h; (f) ClCOCOCI , CH_3OH , 40°C , 4 h; (ii) CH_3ONa , $\text{CH}_3\text{OCH}_2\text{COCl}$, Toluene , 50°C , 2 h (g) 1-phenyl-1H-imidazole, THF 0°C , 1 h, r.t., 24 h.

Table 1. Yields of final desired products.

Entry	Compound ^a	Yield ^b (%)	Entry	Compound ^a	Yield ^b (%)
1	A	55	6	F	53
2	B	61	7	G	69
3	C	56	8	H	49
4	D	48	9	I	49
5	E	57	10	J	51

^aCrossponding to Scheme 4.

^bIsolated yield.

and efficient synthesis of novel molecular scaffolds containing Ritonavir and Lopinavir core and heterocycles as a synthon in the hope to get lead compounds as antiviral agents.

Molecular docking study

The present study focused on the main protease in COVID-19 (PDB ID 6LU7) as the potential for COVID-19 inhibition (Jin et al., 2020).

To find interactions and binding energy between COVID19-Mpro protein and the predicted compounds, a molecular docking was done by AutoDock 4.2 program (Morris et al., 2009). Among the experimental X-ray structures of COVID19-Mpro protein, the crystallographic structure with a PDB entry code of 6LU7 was selected. The first, validation docking on COVID19-Mpro protein and the ligand in X-ray crystallography (**N3**) was done. The analysis of all docked poses showed that the **N3** ligand was located in the binding pocket. The main residues in this pocket were His41, Phe140, Leu141, Asn142, Gly143, Cys145, His163, His164, Met165, Glu166, Leu167, Pro168, Asp187, Arg188, Gln189 and Thr190. The initial coordinates of the ligand were used as the reference and a root-mean-square deviation (RMSD) was obtained between docked ligand and reference at less than 2 Å. Two and three-dimensional analysis for the **N3** ligand is shown in Figure 1.

According to standard drugs (Ritonavir and Lopinavir), novel inhibitors were designed. The molecular docking of the designed ligands with MPro protein was carried out and

the poses of each ligand were ordered in terms of binding energy and clusters (Table 2).

All compounds were perfectly placed in the active site. Among the ten mentioned compounds, structure **A** demonstrated the lowest binding energy, thus it was chosen for further studies. To confirm the stability of compound **A** in the active site of Mpro protein, the MD simulation was performed and also to compare its interaction modes with Lopinavir as a standard drug. Two and three-dimensional analysis for synthesized compounds were shown in Figures S1 and S2.

The compound **A**, Lopinavir and **N3** were superimposed and were shown in Figure S3. It can be seen that compound **A** similar to Lopinavir and **N3** was completely perched into the active site.

The top 3 proposed inhibitors were chosen in terms of energy and main interaction in active site (Figure 2). Figure 2 shows hydrogen bonds between Lopinavir (reference standard) and Ser144, Cys145, Glu166 and Arg188 and pi-alkyl interactions with Met165, Leu167, and Pro168.

Compound **A** forms H-bonds with Mpro protein amino acids Cys145, His164, Glu166 and Gln188 and pi-alkyl interactions with Cys145 and Met165. Compound **B** forms H-bonds with the MPro protein amino acids Asn142, Cys145, Glu166, Gln189, and two sigma and pi interactions with His41.

Compound **C** forms H bonds with the MPro protein amino acids Cys145, Glu166 and Gln189, and pi interaction with His41, also all calculated binding energies using Autodock are shown in Table 2.

Molecular dynamics simulation

According to molecular docking results, compound **A** was chosen for MD simulation. A 100 ns MD simulation was carried out to corroborate the stability of the **A** compound in the Mpro protein active site. Also, interaction modes of compound **A** were compared with a Mpro protein inhibitor as a reference (Lopinavir).

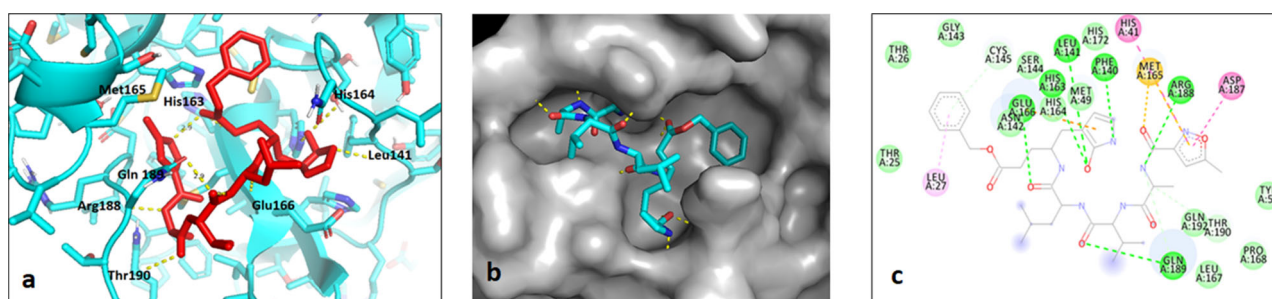


Figure 1. The binding mode of N3 in the active site of COVID19-Mpro protein, obtained from AutoDock4, (a and b) 3D structure, (c) 2D structure.

Table 2. The calculated free binding energies of the designed compounds with COVID19-Mpro protein using Autodock.

Entry	Structures	Binding energy (ΔG) (kcal/mol)	Inhibition constant	Intermolecular energy	Hydrogen bonding and π - π interactions
1	N3	-8.19	990.78 nM	-13.86	Phe140, Leu141, His163, Glu166, His41, Asp187
2	lopinavir	-7.81	1.90 μ M	-13.18	Ser144, Cys145, Glu166, Arg188, His41
3	A	-9.61	90.10 nM	-13.79	Cys145, His164, Glu166, Gln188, His41
4	B	-9.54	101.59 nM	-13.72	Asn142, Cys145, Glu166, Gln189, His41
5	C	-9.32	146.33 nM	-13.50	Cys145, Glu166, Gln189, His41
6	D	-9.20	180.00 nM	-13.38	Asn142, Gly143, Gln189, His163
7	E	-9.19	182.58 nM	-13.37	Gly143, Cys145, Glu166, Thr190
8	F	-9.00	251.28 nM	-13.18	Cys145, Thr190
9	G	-8.88	310.51 nM	-13.65	Gly143, Glu166
10	H	-8.41	686.67 nM	-13.78	Gly143, Glu166
11	I	-8.01	1.35 μ M	-12.78	Thr26, His164, Thr25
12	J	-7.31	4.31 μ M	-13.28	Phe140, Glu166, Gln189, His41, Leu141

Root mean square deviation (RMSD), root-mean-square fluctuation (RMSF), and gyration radius were investigated as the time-dependent behaviors of MD trajectories. To estimate the conformational stability of Mpro protein during the simulation, RMSD of backbone complexes and RMSD of two compounds (compound **A** and Lopinavir) were studied.

As shown in Figure 3(A), in the first 20 ns, the RMSD profile of the Mpro-Lopinavir complex was seen as more stable than Mpro-A complex but in remaining simulation time, the profile of Mpro-A complex was more stable than the Mpro-Lopinavir complex. Generally, RMSD profile did not alter more than 0.28 and 0.38 nm in Mpro-A and Mpro-Lopinavir complexes, respectively. By analysis of the RMSD plots of the two ligands (Figure 3(B)), it can be identified that compound **A** and Lopinavir were superimposed in the second 50 ns simulations. The RMSD profile results show that both ligands had significant stability in the active site during MD simulation.

The compactness of the protein (Rg) was displayed in Figure 4(A). The Rg value of **A** and the Lopinavir were superimposed and the continuity of both complexes was saved during the simulation. The alteration of protein flexibility (RMSF) was investigated during the MD simulation. As shown in Figure 4(B), the RMSF profiles of both complexes were superimposed in all amino acids. The main residues, Cys145 and His163, were seen more stable during MD simulation. Average values of RMSD, RMSF and Rg were calculated 0.333, 0.092 and 2.191, respectively for COVID19-Mpro-A complex. The binding free energy has been also computed for Mpro-Lopinavir and Mpro-A complexes using the g_mmpbsa. The obtained binding energy components are reported in Table 3. As regards of the stability of compound **A** in active site of Mpro-protein, this compound could be propose as COVID-19 Mpro inhibitor.

Experimental section

Chemistry

General synthetic methods: ^1H NMR and ^{13}C NMR spectra were recorded by 400 MHz spectrometer instrument. EI mass spectral analyses were recorded on Shimadzu Japan QP2010S model spectrometer. Thin-layer chromatography (TLC) on silica gel plate was used to checking compounds purity by using hexane and ethyl acetate. The purification process was performed using column chromatography on silica gel (60–120 mesh) by ethyl acetate and hexane mixture as eluent. Details procedures for synthesis and characterization data of products were given in supplementary data.

Molecular docking methods

To find the main interactions and the binding energy of designed compounds with the COVID-19 main protease as a receptor, molecular docking was done by AutoDock 4.2 program (Morris et al., 2009). The pdb file of COVID-19 main proteases was taken from the Protein Data Bank (PDB ID: 6LU7). All water molecules, ligand, and ions were removed from pdb file. Then polar hydrogens were added and the partial atomic charge was calculated by Kollman method. Then the prepared file was saved in pdbqt format to use in the following steps. Three-dimensional structures of designed compounds were depicted in Marvin Sketch Ver. 5.7, ChemAxon (Cosconati et al., 2010). The partial charges of atoms were determined according to the Gasteiger-Marsili procedure, and non-polar hydrogens of the compounds were merged (Morris et al., 1998). A $50 \times 50 \times 50 \text{ \AA}$ (x, y, and z) grid box was centered on the protease binding pocket with a 0.375 nm spacing for each dimension. Docking was

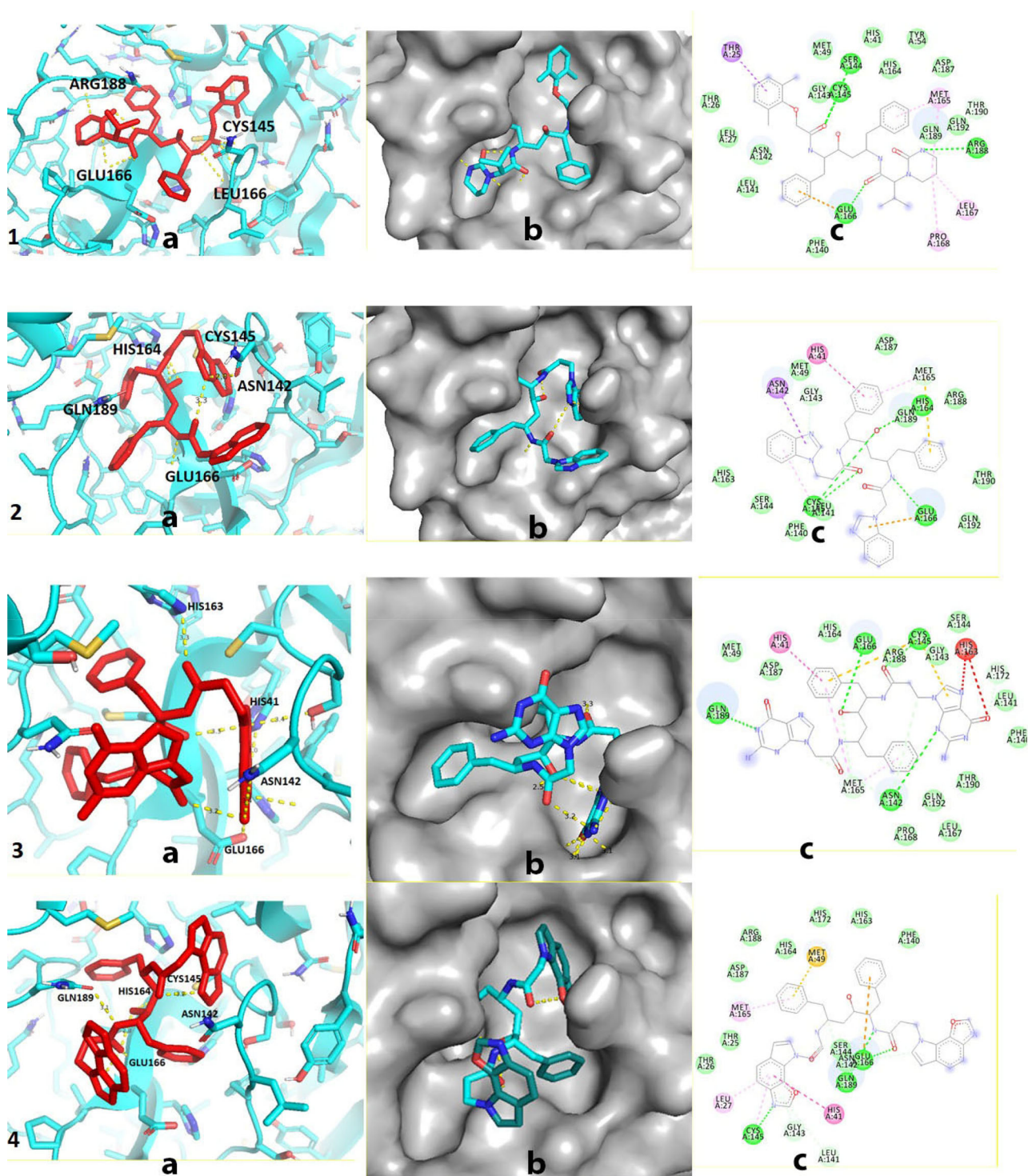


Figure 2. The binding mode of Lopinavir, A, B and C (1, 2, 3 and 4 respectively) in the active site of COVID19-Mpro protein, obtained from AutoDock4; 3D structures and 2D structure.

performed by Lamarckian genetic algorithm and empirical scoring function by using a flexible method. The program was run for a total number of 50 Genetic algorithm runs. Eventually, the docking procedure was carried out by AutoDock 4.2. All of the runs were ranked in term of the binding energy and were analyzed to obtain the best conformation and orientation of the ligand in the active site of the protein. Visualization of docking results has been done

by Discovery Studio visualizer version 17.2 and Pymol version 1.1level (Dassault Systèmes BIOVIA, 2016).

Molecular dynamics simulation methods

The best-ranked nominee from docking results was considered for evaluating their thermodynamic behavior and

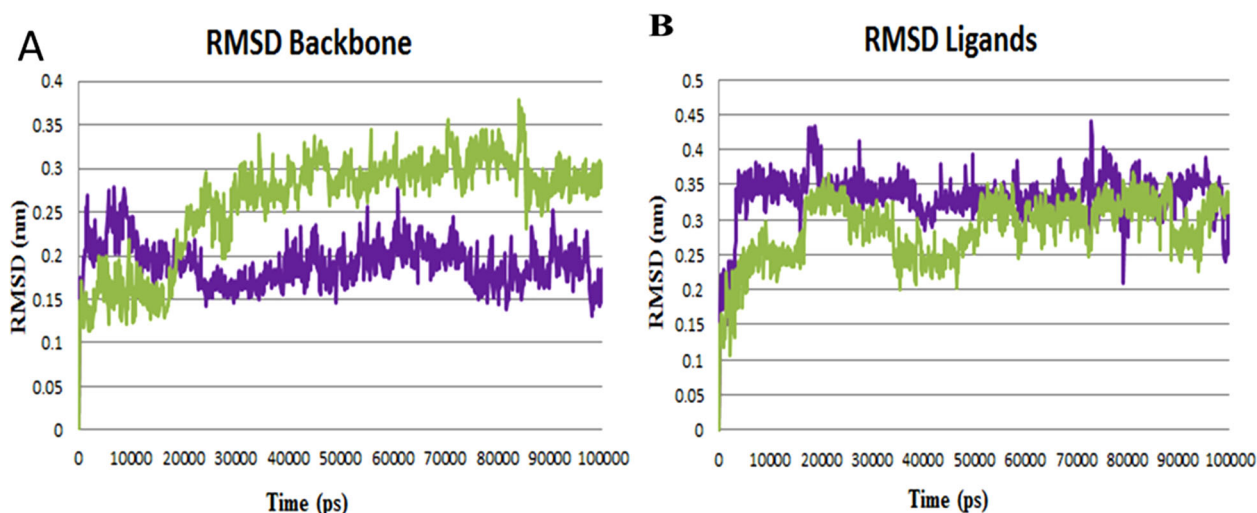


Figure 3. RMSD plots of COVID19-Mpro protein inhibitors as a function of simulation time. (A) RMSD of backbone atoms of COVID19-Mpro-A (purple) and COVID19-Mpro-Lopinavir (green) complexes. (B) RMSD plot of Compound A and Lopinavir.

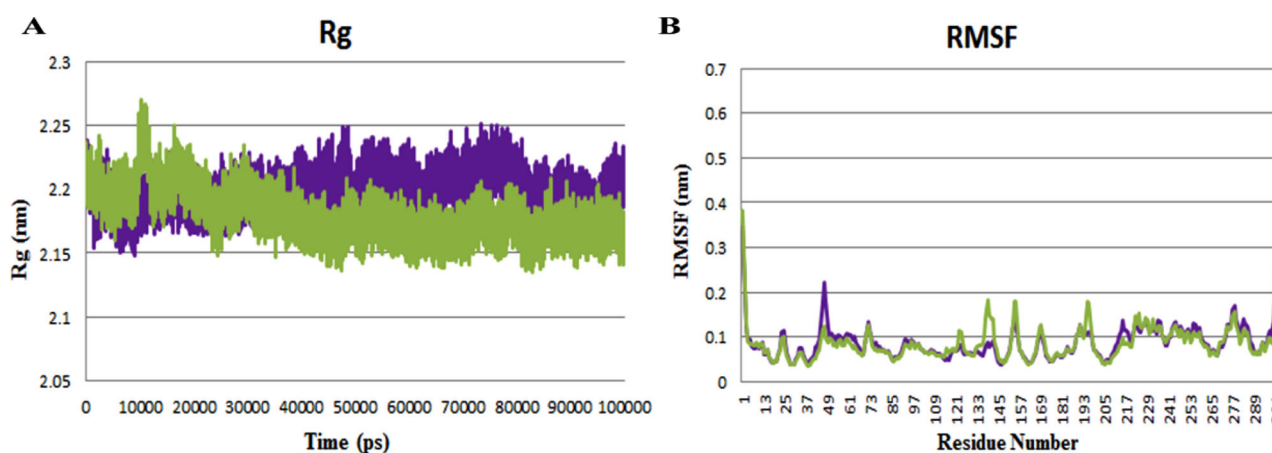


Figure 4. (A) The gyration radius plot of Mpro-Lopinavir (green) and A (purple). (B) The RMSF plot of Mpro-Lopinavir (green) and A (purple).

Table 3. The binding energy components obtained from g_mmpbsa.

Complex	$\Delta G_{\text{binding}}^a$	$\Delta G_{\text{polar}}^b$	$\Delta G_{\text{nonpolar}}^c$	ΔE_{elec}^d	ΔE_{vdW}^e
Mpro-Lopinavir	-90.310 ± 7.565	162.973 ± 8.611	-21.976 ± 0.783	-47.603 ± 6.208	-200.705 ± 11.742
Mpro-A	-75.878 ± 9.078	134.881 ± 6.582	-20.441 ± 0.611	-7.741 ± 5.286	-182.577 ± 9.024

^aBinding energy.

^bPolar solvation energy.

^cNon-polar solvation energy.

^dElectrostatic component to the binding energy in kcal/mol.

^eVan der Waals component to the binding energy in kcal/mol.

stability of binding mode in the Mpro binding pocket using molecular dynamics (MD) simulation studies. All MD simulations were accomplished by GROMACS-2019.3 package (Abraham et al., 2015). The Amber 99.sb force field was engaged in MD simulations (Cornell et al., 1995). Drug topology parameters were ready by the AnteChamber Python Parser InterfAcE (ACYPPE) (Da Silva & Vranken, 2012). To characterize which residue adopts non-standard ionization states, was obtained pKa values using PROPKA 3.1 webserver (Søndergaard et al., 2011). A TIP3P water model was select (Jorgensen, 1983) and the complex of ligand-protein was soaked in a dodecahedron water box. Some cations, Na⁺ ions, were substituted with solvent water molecules to neutralizing the system. The energy minimization was performed and MD simulation was commenced by two stages of the process: 1) 500 ps simulation in the NVT

ensemble at a constant number of particles, volume, and temperature; 2) 1 ns simulation in the NPT ensemble at a constant number of particles, pressure, and temperature. Finally, MD simulation was run at 300 K temperature for 100 ns. The Particle Mesh Ewald (PME) method and the linear constraint (LINCS) algorithm were carried out to computing long-range electrostatic interactions and covalent bond constraints, respectively. Structure visualization was done using VMD 1.8.6 (Humphrey et al., 1996) and PyMOL Tcl.

Conclusion

In summary, we designed and synthesized novel potential COVID-19 main protease inhibitors that contain the main

core of Lopinavir connected to various heterocyclic fragments. Lopinavir is one of the rare successful clinical trial agents for the treatment of COVID-19 patients. First, molecular docking was carried out to identify the interactions of these compounds with the main protease protein. Our findings revealed that all designed structures were docked successfully but compound **A** exhibited the lowest binding energy within the protein pocket and could be considered as a potential of COVID-19 main protease inhibition. The molecular dynamic simulation was also confirmed our claim. Next, these structures were synthesized through facile and efficient six-step reactions instead of some available strategies which contain more than ten harsh reaction steps. Because of the similarity of these synthesized compounds to Lopinavir and Ritanivir scaffold, they could be introduced as potential of main protease inhibition. However, further research is needed to investigate the validation of these compounds using in vitro and in vivo methods to pave a way for these compounds in drug discovery.

Acknowledgements

This work was financially supported by Isfahan Pharmaceutical Sciences Research Center, School of Pharmacy, Isfahan University of Medical Sciences, Isfahan, Iran.

Disclosure statement

No potential conflict of interest was reported by the author(s).

ORCID

Maryam Abbasi  <http://orcid.org/0000-0002-3022-2507>

References

- Abraham, M. J., Murtola, T., Schulz, R., Páll, S., Smith, J. C., Hess, B., & Lindahl, E. (2015). GROMACS: High performance molecular simulations through multi-level parallelism from laptops to supercomputers. *SoftwareX*, 1-2, 19–25. <https://doi.org/10.1016/j.softx.2015.06.001>
- Bhaskar, G., Kumar, A. R., Ramu, E., & Rao, B. V. (2008). Synthesis of a hydroxyethylene dipeptide isostere, a core unit of the HIV protease inhibitors ritonavir and lopinavir, and its C-5 epimer. *Synthesis*, 2008(19), 3061–3064. <https://doi.org/10.1055/s-2008-1067252>
- Chern, J. W., Lee, H. Y., Chen, C. S., Shewach, D. S., Daddona, P. E., & Townsend, L. B. (1993). Nucleosides. 5. Synthesis of guanine and formycin B derivatives as potential inhibitors of purine nucleoside phosphorylase. *Journal of Medicinal Chemistry*, 36(8), 1024–1031. <https://doi.org/10.1021/jm00060a010>
- Cornell, W. D., Cieplak, P., Bayly, C. I., Gould, I. R., Merz, K. M., Ferguson, D. M., Spellmeyer, D. C., Fox, T., Caldwell, J. W., & Kollman, P. A. (1995). A second-generation force field for the simulation of proteins, nucleic acids, and organic molecules. *Journal of the American Chemical Society*, 117(19), 5179–5197. <https://doi.org/10.1021/ja00124a002>
- Cosconati, S., Forli, S., Perryman, A. L., Harris, R., Goodsell, D. S., & Olson, A. J. (2010). Virtual screening with AutoDock: Theory and practice. *Expert Opinion on Drug Discovery*, 5(6), 597–607. <https://doi.org/10.1517/17460441.2010.484460>
- Cunningham, A. C., Goh, H. P., & Koh, D. (2020). Treatment of coronavirus disease 2019 in Shandong, China: A cost and affordability analysis. *Infectious Diseases of Poverty*, 24, 91.

- Damo, I. A., Benedetti, F., Berti, F., & Campaner, P. (2006). Stereoselective hydroazidation of amino enones: synthesis of the ritonavir/lopinavir core. *Organic Letters*, 8(1), 51–54. <https://doi.org/10.1021/ol0524104>
- Da Silva, A. W. S., & Vranken, W. F. (2012). ACPYPE - AnteChamber Python Parser interface. *BMC Research Notes*, 5, 367. <https://doi.org/10.1186/1756-0500-5-367>
- Dassault Systèmes BIOVIA. (2016). *Discovery studio modeling environment, Release 2017 (Version 17.2)* [software]. Dassault Systèmes. <https://www.3dsbiovia.com/products/collaborative-science/biovia-discovery-studio>;
- Dumas, D. J. (1999). *Process for the preparation of sulfentrazone* (US Patent 5990315).
- Elfiky, A. A., Mahdy, S. M., & Elshemey, W. M. (2017). Quantitative structure-activity relationship and molecular docking revealed a potency of anti-hepatitis C virus drugs against human corona viruses. *Journal of Medical Virology*, 89(6), 1040–1047. <https://doi.org/10.1002/jmv.24736>
- Fan, H., Peng, J., Hamann, M. T., & Hu, J.-F. (2008). Lamellarins and related pyrrole-derived alkaloids from marine organisms. *Chemical Reviews*, 108(1), 264–287. <https://doi.org/10.1021/cr078199m>
- Ghosh, R., Chakraborty, A., Biswas, A., & Chowdhuri, S. (2020). Identification of polyphenols from *Broussonetia papyrifera* as SARS CoV-2 main protease inhibitors using in silico docking and molecular dynamics simulation approaches. *Journal of Biomolecular Structure and Dynamics*, 12, 1.
- Hall, D. C., Jr, & Ji, H. F. (2020). COVID-19: Travel health and the implications for sub-Saharan Africa. *Travel Medicine and Infectious Disease*, 35, 101646. <https://doi.org/10.1016/j.tmaid.2020.101646>
- Hassan, A. E., Abdella, M. M., & Ahmed, A. I. (1997). Studies on synthesis and cyclization reactions 2-(5-Amino-3-arylpyrazol-1-yl)-3-methylquinolines. *Journal of Chemical Research*, 5, 322.
- Hemida, M. G., & Alnaeem, A. (2019). Some One Health based control strategies for the Middle East respiratory syndrome coronavirus. *One Health (Amsterdam, Netherlands)*, 8, 100102. <https://doi.org/10.1016/j.onehlt.2019.100102>
- Hřebabecký, H., Dejmeš, M., Dračinský, M., Šála, M., Leyssen, P., Neyts, J., Kaniaková, M., Krůšek, J., & Nencka, R. (2012). Synthesis of novel azanorbornylpurine derivatives. *Tetrahedron*, 68(4), 1286–1298. <https://doi.org/10.1016/j.tet.2011.11.035>
- Humphrey, W., Dalke, A., & Schulten, K. (1996). VMD: Visual molecular dynamics. *Journal of Molecular Graphics*, 14(1), 33–38. [https://doi.org/10.1016/0263-7855\(96\)00018-5](https://doi.org/10.1016/0263-7855(96)00018-5)
- Imbri, D., Tauber, J., & Opatz, T. (2014). Synthetic approaches to the lamellarins—a comprehensive review. *Marine Drugs*, 12(12), 6142–6177. <https://doi.org/10.3390/md12126142>
- Jin, Z., Du, X., Xu, Y., Deng, Y., Liu, M., Zhao, Y., Zhang, B., Li, X., Zhang, L., Peng, C., Duan, Y., Yu, J., Wang, L., Yang, K., Liu, F., Jiang, R., Yang, X., You, T., Liu, X., ... Yang, H. (2020). Structure of Mpro from SARS-CoV-2 and discovery of its inhibitors. *Nature*, 582(7811), 289–293. <https://doi.org/10.1038/s41586-020-2223-y>
- Jorgensen, W. (1983). Comparison of simple potential functions for simulating liquid water. *Journal of Chemical Physics*, 79, 793.
- Kadil, Y., Mouhcine, M., & Filali, H. (2020). In silico study of pharmacological treatments against SARS-CoV2 main protease. *Journal of Pure and Applied Microbiology*, 14(suppl 1), 1065–1071. <https://doi.org/10.22207/JPAM.14.SPL1.45>
- Khoobi, M., Ghanoni, F., Nadri, H., Moradi, A., Pirali Hamedani, M., Homayouni Moghadam, F., Emami, S., Vosooghi, M., Zadnabad, R., Foroumadi, A., & Shafiee, A. (2015). New tetracyclic tacrine analogs containing pyrano[2,3-c]pyrazole: efficient synthesis, biological assessment and docking simulation study. *European Journal of Medicinal Chemistry*, 89, 296–303. <https://doi.org/10.1016/j.ejmech.2014.10.049>
- Ko, W. C., Rolain, J. M., Lee, N. Y., Chen, P. L., Huang, C. T., Lee, P. I., & Hsueh, P. R. (2020). Arguments in favour of remdesivir for treating SARS-CoV-2 infections. *International Journal of Antimicrobial Agents*, 9, 78.
- Kumar, A., Voet, A., & Zhang, K. Y. J. (2012). Fragment Based Drug Design: From Experimental to computational approaches. *Current Medicinal Chemistry*, 19(30), 5128–5147. <https://doi.org/10.2174/092986712803530467>
- Min, G., Eric, C., & Lihu, Y. (2006). Potential purine antagonists. VI. Synthesis of 1-Alkyl- and 1-Aryl-4-substituted Pyrazolo[3,4-d] pyrimidines. *Tetrahedron Letters* 47, 5797.

- Morales, P. R., MacGregor, A. J., Kanagarajah, K., Patel, S., & Schlagenhauf, P. (2020). Going global - Travel and the 2019 novel coronavirus. *Travel Medicine and Infectious Disease*, 33, 101578. <https://doi.org/10.1016/j.tmaid.2020.101578>
- Morris, G. M., Goodsell, D. S., Halliday, R. S., Huey, R., Hart, W. E., Belew, R. K., & Olson, A. J. (1998). Automated docking using a Lamarckian genetic algorithm and an empirical binding free energy function. *Journal of Computational Chemistry*, 19(14), 1639–1662. [https://doi.org/10.1002/\(SICI\)1096-987X\(19981115\)19:14<1639::AID-JCC10>3.0.CO;2-B](https://doi.org/10.1002/(SICI)1096-987X(19981115)19:14<1639::AID-JCC10>3.0.CO;2-B)
- Morris, G. M., Huey, R., Lindstrom, W., Sanner, M. F., Belew, R. K., Goodsell, D. S., & Olson, A. J. (2009). AutoDock4 and AutoDockTools4: Automated docking with selective receptor flexibility. *Journal of Computational Chemistry*, 30(16), 2785–2791. <https://doi.org/10.1002/jcc.21256>
- Murray, C. W., & Blundell, T. L. (2010). Docking and ligand binding affinity: Uses and pitfalls. *Current Opinion in Structural Biology*, 20(4), 497–507. <https://doi.org/10.1016/j.sbi.2010.04.003>
- Sgrignani, J., & Magistrat, A. (2012). Influence of the membrane lipophilic environment on the structure and on the substrate access/egress routes of the human aromatase enzyme. A computational study. *Journal of Chemical Information and Modeling*, 52(6), 1595–1606. <https://doi.org/10.1021/ci300151h>
- Søndergaard, C. R., Olsson, M. H., Rostkowski, M., & Jensen, J. H. (2011). Improved treatment of ligands and coupling effects in empirical calculation and rationalization of pKa values. *Journal of Chemical Theory and Computation*, 7(7), 2284–2295. <https://doi.org/10.1021/ct200133y>
- Speck-Planche, A., Luan, F., & Cordeiro, M. N. (2012). Role of ligand-based drug design methodologies toward the discovery of new anti-Alzheimer agents: Futures perspectives in fragment-based ligand design. *Current Medicinal Chemistry*, 19(11), 1635–1645. <https://doi.org/10.2174/092986712799945058>
- Stoner, E. J., Cooper, A., Dickman, D. A., Kolaczowski, L., Lallaman, J. E., Liu, J. H., Oliver-Shaffer, P. A., Patel, K. M., Paterson, J. B., Plata, D. J., Riley, D. A., Sham, H. L., Stengel, P. J., & Tien, J. H. J. (2000). Synthesis of HIV protease inhibitor ABT-378 (lopinavir). *Organic Process Research & Development*, 4(4), 264–269. <https://doi.org/10.1021/op990202j>
- Suvannang, N., Nantasenamat, C., Isarankura-Na-Ayudhya, C., & Prachayasittikul, V. (2011). Molecular docking of aromatase inhibitors. *Molecules*, 16(5), 3597–3617. <https://doi.org/10.3390/molecules16053597>
- Tănase, C. I., Drăghici, C., Căproiu, M. T., Shova, S., Mathe, C., Cocu, F. G., Enache, C., & Maganu, M. (2014). New carbocyclic nucleoside analogues with a bicyclo[2.2.1]heptane fragment as sugar moiety; synthesis, X-ray crystallography and anticancer activity. *Bioorganic & Medicinal Chemistry*, 22(1), 513–522. <https://doi.org/10.1016/j.bmc.2013.10.056>
- Weng, J. Q., Wang, L., & Liu, X. H. (2012). Crystal structure of 2-(pyridin-4-yl)-5-(undecylthio)-1,3,4-oxadiazole. *Journal of the Chemical Society of Pakistan*, 34, 1248.
- WHO. (2016). Middle East respiratory syndrome coronavirus (MERS-CoV). [http:// who.int](http://who.int)
- WHO. (2020). *Coronavirus disease 2019 (covid-19): Situation report*, Vol. 74. <http:// who.int>
- Zhou, P., Yang, X.-L., Wang, X.-G., Hu, B., Zhang, L., Zhang, W., Si, H.-R., Zhu, Y., Li, B., Huang, C.-L., Chen, H.-D., Chen, J., Luo, Y., Guo, H., Jiang, R.-D., Liu, M.-Q., Chen, Y., Shen, X.-R., Wang, X., ... Shi, Z.-L. (2020). A pneumonia outbreak associated with a new coronavirus of probable bat origin. *Nature*, 579(7798), 270–273. <https://doi.org/10.1038/s41586-020-2012-7>